Segmentation of optical remote sensing images for detecting homogeneous regions in space and time

Wanderson S. Costa[1], Leila M. G. Fonseca[1], Thales S. Körting[1], Margareth G. Simões[2], Hugo N. Bendini[1], Ricardo C. M. Souza[1]

[1]Instituto Nacional de Pesquisas Espaciais (INPE)
ZIP Code 12227-010 – São José dos Campos – SP – Brazil

[2]Embrapa Solos, Rua Jardim Botânico, 1024
ZIP Code 22460-000 – Rio de Janeiro – RJ – Brazil

{wanderson.costa, leila.fonseca, thales.korting}@inpe.br,
margareth.simoes@embrapa.br, hugo.bendini@inpe.br, cartaxo@dpi.inpe.br

Abstract. *With the amount of multitemporal and multiresolution images growing exponentially, the number of image segmentation applications is recently increasing and, simultaneously, new challenges arise. Hence, there is a need to explore new segmentation concepts and techniques that make use of the temporal dimension. This paper describes a spatio-temporal segmentation that adapts the traditional region growing technique to detect homogeneous regions in space and time in optical remote sensing images. Tests were conducted by considering the Dynamic Time Warping measure as the homogeneity criterion. Study cases on high temporal resolution for sequences of MODIS and Landsat-8 OLI vegetation indices products provided satisfactory outputs and demonstrated the potential of the spatio-temporal segmentation method.*

1. Introduction

Satellite image analysis is a key role for detecting land use/cover changes in different biomes. The extensive amount of remote sensing data, combined with information from ecosystem models, offers a good opportunity for predicting and understanding the behaviour of terrestrial ecosystems [Boriah 2010]. As satellite products have a repetitive data acquisition and its digital format is suitable for computer processing, remote sensing data have become the main source for application of change detection and observation of land use and land cover during the last decades [Lambin and Linderman 2006].

If the image analysis is performed using only per-pixel techniques, inherent information of the objects in the scene are discarded, such as shape, area and statistical parameters. In order to exploit these information, there are segmentation algorithms, which partition images in regions whose pixels present similar properties [Blaschke 2010, Bins et al. 1996]. Using a homogeneity criterion between the image pixels, the identified regions are treated as objects from which characteristics can be extracted to be used in the analysis. Consequently, the result of the segmentation reduces the volume of data to be studied in the analysis, regarding the number of elements to be analysed.

Several segmentation techniques applied in change detection are still derived from the traditional snapshot model [Dey et al. 2010], that analyses each time step independently. However, a thorough literature review revealed a record of few stud-

ies that adapted methods based on objects for applications with multitemporal data [Thompson and Lees 2014].

Change detection based on time series is advantageous compared to the pure observation of image sequences, since the series takes into account information regarding temporal dynamics and changes in the landscape rather than just observing the differences between two or more images collected on different dates [Boriah 2010]. Continuous observations from remote sensors provide high temporal and spatial resolution imagery, and better remote sensing image segmentation techniques are mandatory for efficient analysis [Schiewe 2002, Dey et al. 2010]. Nonetheless, a large amount of temporal data has been generated over the past years, which forces the remote sensing community to rethink processing strategies for satellite time series analysis and visualization [Freitas et al. 2011].

In this paper, we describe a segmentation method applied to time series of Earth Observation data. The method integrates regions in order to detect objects that are homogeneous in space and time. This approach aims to overcome the limitations of the snapshot model, adapting the well known segmentation method based on spatial region growing [Adams and Bischof 1994]. Study cases were conducted using time series of MODIS and Landsat-8 OLI scenes by applying spatio-temporal segmentation using the Dynamic Time Warping measure [Sakoe and Chiba 1971] as the homogeneity criterion.

2. Remote Sensing Image Segmentation

One of the first steps in every remote sensing image analysis, segmentation is a basic and critical task in image processing whereby the image is partitioned into regions, also called objects, whose pixels are similar considering one or more properties [Haralick and Shapiro 1985]. Overall, it is expected that the objects of interest are automatically extracted as a result of segmentation. Features can be extracted from these objects and used later for data analysis.

However, segmentation algorithms generally do not yield a perfect partition of the scene, producing segments that divide the targets of interest into several regions (over-segmentation) or generate regions containing more than one target (under-segmentation). By applying segmentation methods for remote sensing data, both of the aforementioned results may happen within a single scene, depending on the heterogeneity of the objects that are taken into account [Schiewe 2002]. In addition, many segmentation algorithms are directed to a reduced class of problems or data. Errors and distortions in the segmentation process are reflected in the subsequent steps, including classification.

The region growing algorithm [Adams and Bischof 1994] is one of the most applied segmentation techniques in remote sensing image processing. The method groups pixels or sub-regions into larger regions depending on how they are similar or not, using some similarity criteria. The technique starts with a set of pixels called *seeds* and, from them, grows regions by adding neighbour pixels with similar properties.

The threshold definitions in region growing segmentation are a key step due to their direct influence on the accuracy of the output. The similarity threshold analyses if the pixel value difference or the average difference of a set of neighbouring pixels is smaller than a given threshold. This value supports the user to control the segmentation result in an interactive way, depending on the goal and study area [Oliveira 2002].

Furthermore, it is reported that there is not an optimal threshold value, since it depends on the image type, land cover, the period in which the data was collected and research purposes. In general, the threshold is reached after several tests among possible combinations of the algorithm. The tests continue until the result of the segmentation is suitable for a particular purpose [Oliveira 2002].

Many of the recent segmentation processes based on objects have paid attention to high image spatial resolutions whereas, so far, there are few studies adapted to multitemporal data [Thompson and Lees 2014]. Most of the change detection analysis uses the well-known snapshot model [Haralick and Shapiro 1985], observing only the differences between discrete dates [Dey et al. 2010, De Chant and Kelly 2009, Duro et al. 2013, Gómez et al. 2011]. Additionally, most of the object-based multitemporal analysis performs inferences about the nature of the changes *after* the image processing, that is, the understanding of the phenomenon changes is inferred by measuring the number and the magnitude of the observed differences in the objects after the change.

Some object-based techniques aim at performing the segmentation generating one output for each instant of time and then comparing the objects changes over time [Im et al. 2008, Niemeyer et al. 2008, Gómez et al. 2011]. In other studies, the objects are defined in the first image, and then their differences are analysed in subsequent image [Blaschke 2005, Pape and Franklin 2008, Duro et al. 2013].

Another approach has included the time as an additional factor within the segmentation, being used with the spatial and spectral image features [Thompson and Lees 2014]. However, many studies that applies this segmentation approach have used a limited number of multitemporal images [Bontemps et al. 2008, Desclée et al. 2006, Drăguţ et al. 2010, Drăguţ et al. 2014] and they did not make use of time series of high temporal resolution images [Dey et al. 2010]. A direct characterization of changes in a phenomenon requires that the observations are done *during* the change process [Thompson and Lees 2014], which can be exploited through high temporal resolution images.

3. Satellite Image Time Series

Satellite image time series (SITS) offer new perspectives for the understanding of ocean, land and atmospheric changes by identifying the factors that cause these modifications and predicting future changes [Boriah 2010]. The time component integrated with spatial and spectral properties of the images can result in a rich source of information that, if properly explored, reveals complex and important patterns found on the environment, including the land and ocean dynamics [Bruzzone et al. 2003].

SITS are relevant data in the study of dynamic phenomena and the interpretation of their evolution over time [Boulila et al. 2011]. The time series of vegetation indices, for example, can be used to analyse seasonality for cover monitoring purposes. Vegetation indices represent improved measures of spatial, spectral and radiometric surface vegetation conditions [Tucker et al. 2005]. In the analysis and characterization of vegetation cover, for example, vegetation indices are used for seasonal and inter-annual monitoring of biophysical, phenological and structural vegetation parameters [Huete et al. 2002]. Fig. 1 shows the time series generation for a pixel $p(x, y)$. For each pixel, a time series can be observed, representing the pixel value variation over time.

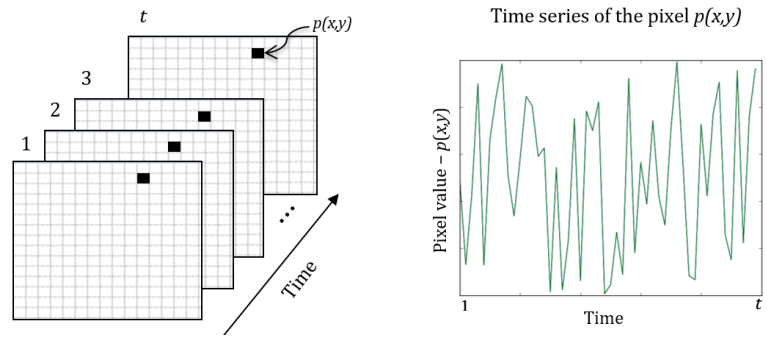

Figure 1. Example of a time series for the pixel $p(x, y)$.

One of most used vegetation indices is the NDVI (Normalized Difference Vegetation Index) [Justice et al. 2002] and its calculation is based on the reflectance of red and near-infrared wavelengths [Tucker 1979]. The band ratio in the calculation of NDVI reduces some forms of noise, such as the lighting differences, cloud shadows and topographical variations. However, this index has low sensitivity in regions with high concentration of biomass and may have limitations related to soil brightness variations [Jiang et al. 2008].

3.1. Dynamic Time Warping

Dynamic Time Warping (DTW) is one of the most used measures to quantify the similarity between two time series [Petitjean et al. 2012]. Originally designed to treat automatic speech recognition [Sakoe and Chiba 1971, Sakoe and Chiba 1978], DTW measures the optimal global alignment between two time series and exploits temporal distortions between them.

The choice for a good similarity measure plays a key role since it defines the way to treat the temporality of data. The main change detection analysis in remote sensing images consists in comparing the data to estimate the similarity between them [Petitjean et al. 2011]. In many cases, the similarity is computed using a distance measure between two instances.

Among the known distances, DTW has the ability to realign two time series, so that each element of the first series is associated with at least one of the second series. With DTW, two time series out of phase can be aligned in a nonlinear form (Fig. 2). Providing the cost of this alignment, DTW highlights similarities that the Euclidean distance is not able to capture, comparing shifted or distorted time series [Petitjean et al. 2011].

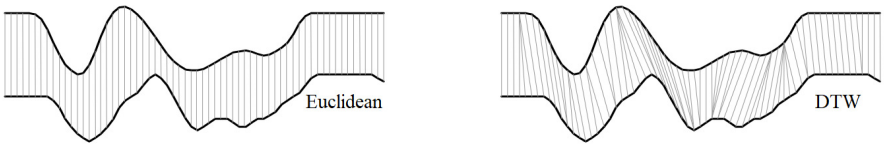

Figure 2. Although the two series have similar shapes, they are not aligned in the time axis. DTW nonlinear alignment allows a more intuitive distance to be calculated. Source: Adapted from [Chu et al. 2002].

Let A and B be two time series of length M and N, respectively, where $A = \langle a_1, a_2, \cdots, a_M \rangle$ and $B = \langle b_1, b_2, \cdots, b_N \rangle$. The first step for calculating the DTW measure between A and B is to build a matrix of size $M \times N$, where each matrix element (i, j) corresponds to a distance measured between a_i and b_i. This distance, $\delta(a_i, b_j)$ can be computed using different metrics, such as the absolute difference $d(a_i, b_i) = |a_i - b_i|$ or the Euclidean distance. The matrix can be recursively calculated by (Eq. 1):

$$D\left(a_i, b_j\right) = \delta\left(a_i, b_j\right) + \min \begin{cases} D\left(a_{i-1}, b_{j-1}\right), \\ D\left(a_i, b_{j-1}\right), \\ D\left(a_{i-1}, b_j\right) \end{cases} \tag{1}$$

Matrix elements are calculated from left to right and from bottom to top. The algorithm adds the distance value δ of the elements in that position of each series. The elements receive the lowest value from the previous adjacent elements to the left, down and diagonal. Once the matrix is completely filled, the last element at bottom right gives the value of the best alignment of the two time series.

DTW measure has been the subject of studies for analysis of SITS. Some researches, for example, used DTW as a tool to treat problems related to comparing time series of different sizes and irregular samples containing cloud cover [Petitjean et al. 2011, Petitjean et al. 2012]. Another study presented a weighted version of DTW for land cover and land use classification [Maus et al. 2016].

4. Methodology

The proposed spatio-temporal segmentation by region growing is diagrammed in Fig. 3. The algorithm can be expressed by the following steps:

1. Select a sequence of images as input data.
2. Determine the number and location of the seeds at the image.
3. Compute DTW distance between the time series of the seeds and their neighbors. The similar neighbors are added to the region.
4. Continue examining all the neighbors until no similar neighbor is found. Label the obtained segmented as a complete region.
5. Observe the next unlabelled seed and repeat the process until all the seeds or pixels are labelled in a region.

The core of our methodology is to use DTW measure as the homogeneity criterion for growing regions in the study cases. These time series were used in DTW calculation between the seeds and its neighbouring pixels. The segmentation algorithm was written using R language.

For the acceptance or rejection of a given threshold in a remote sensing image segmentation result, the resulting segments were compared with a remote sensing image at the same location of the scene in the end of the time series. The similarity threshold was reached using the same seed set in all tests. The segmentation result can also be compared visually with a reference map, previously set by photo-interpretation.

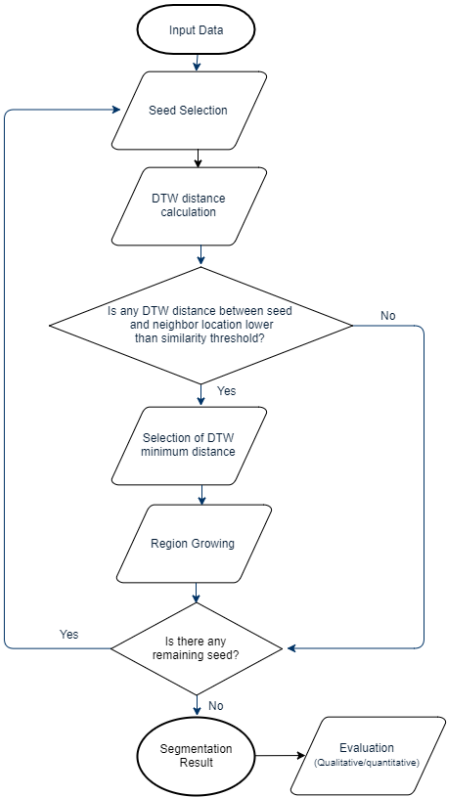

Figure 3. Flowchart of the proposed methodology.

5. Results and Discussion

Our technique was used to evaluate two central-western areas in Brazil. The first test was conducted using NDVI MODIS scenes, with spatial resolution of 250 m. The study area is located in the state of Mato Grosso (MT) and covers 250,000 km^2, illustrated in Fig. 4. We used 92 NDVI scenes between January 2010 and December 2013, with temporal resolution of 16 days. The NDVI produced by MODIS images were retrieved from atmosphere-corrected bidirectional surface reflectance.

This test aimed to illustrate the utility of the method for large areas. The area contains regions of large croplands and native vegetation areas. Since the spatial resolution of the images is low, the expected segmentation output includes large segmented areas with similar geo-objects presenting homogeneity over time. The similarity threshold was defined empirically, based on visual inspection of the results. For the segmentation result presented in Fig. 5, the similarity threshold was set to 0.05. The processing time was approximately 4 hours.

Evaluating the result of an image segmentation is difficult because currently no standard assessment techniques exist [Eeckhaut et al. 2012]. For this test, we compared the segmentation result to a Landsat-8 image, evaluating the output based on photo-interpretation of the satellite image. As shown in Fig. 5, the segmentation distinguished regions corresponding to native vegetation, croplands and urban areas. Visually, the image objects represented similar-sized groups of geo-objects, such as trees, residential areas

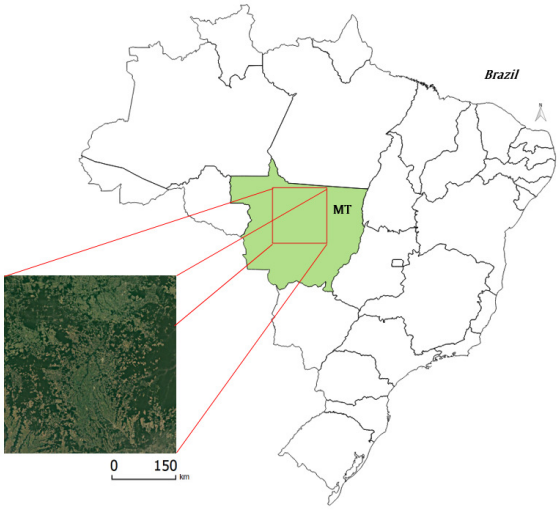

Figure 4. Study area for the first test. Landsat-8 (R4G3B2) imagery of the study area.

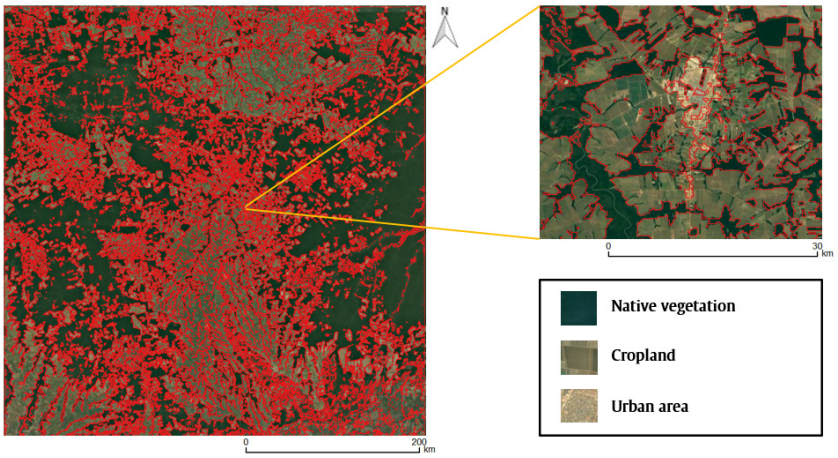

Figure 5. Segmentation output (red outlines) for the first test. The segments are superimposed on a Landsat-8 image (R4G3B2). The zoomed area shows that the algorithm distinguished native vegetation, croplands and urban areas.

and agricultural fields.

In the second test, the study area covers a central area in the state of Goiás, located in Santo Antônio de Goiás City, illustrated in Fig. 6. A sequence of 44 images obtained from NDVI Landsat-8 OLI between November 12, 2014 and September 30, 2016 were used, with temporal resolution of 16 days. All images have a dimension of 189×161 pixels, with spatial resolution of 30 m.

In this test, we used 10 reference polygons as ground truth provided by Brazilian Agricultural Research Corporation (EMBRAPA) [Brazil 2011]. This subset of 10 polygons were chosen because they were regions with homogeneous properties in the described period, also according to information provided by EMBRAPA (see Table 1). The

similarity threshold was chosen so that the agricultural, pasture and forest areas could be separated from the other neighboring targets.

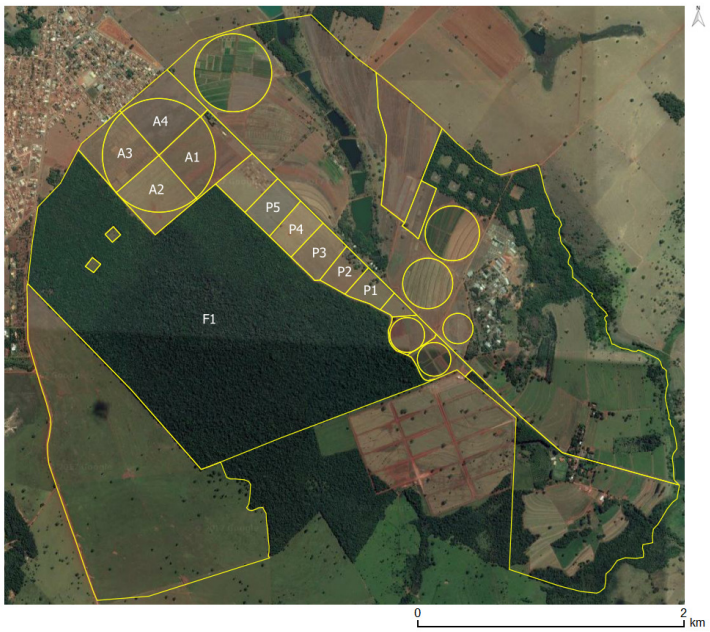

Figure 6. Study area for the second test using Landsat-8 OLI scenes. The yellow outlines are polygons provided by EMBRAPA. The labelled polygons (A1, A2, A3, A4, P1, P2, P3, P4, P5 and F1) were used as ground truth.

Table 1. Land use description of each labelled polygon for each harvest/winter.

Label	Harvest (2014/2015)	Winter (2015)	Harvest (2015/2016)	Winter (2016)
P1	pasture	pasture	pasture	pasture
P2	pasture	pasture	pasture	pasture
P3	soybean	fallow	rice	fallow
P4	rice	fallow	maize + brachiaria	pasture
P5	pasture	pasture	soybean	fallow
A1	maize + brachiaria	pasture	soybean	fallow
A2	rice	fallow	maize + brachiaria	fallow
A3	soybean	fallow	rice	pasture
A4	pasture	pasture	soybean	fallow
F1	forest	forest	forest	forest

Also in this experiment, the similarity threshold was defined empirically, in this case set to 0.045. The processing time was 183 seconds. The segmentation result is shown in Fig. 7. Visually, the proposed method was able to create similar-shaped segments compared to the reference polygons. To evaluate this result, the segmented regions were visually compared to reference polygons.

Visually, the segmented polygons represented regions of similar size to the reference polygons P3, P4, P5, and F1. However, the segmented polygon that corresponds to

P1 presented similar behavior to its neighboring polygon during the two analyzed years. The algorithm considered the two polygons as a single area with homogeneous properties in the observed period. A similar case occurred with polygons A1 and A4. As can be seen in Table 1, the two areas have the same type of land use, differing only in the harvest (2014/2015). The method considered the two areas as a single region. However, the references A2 and A3 were the ones that most diverged from the algorithm result, since each one of them were separated into two distinct regions.

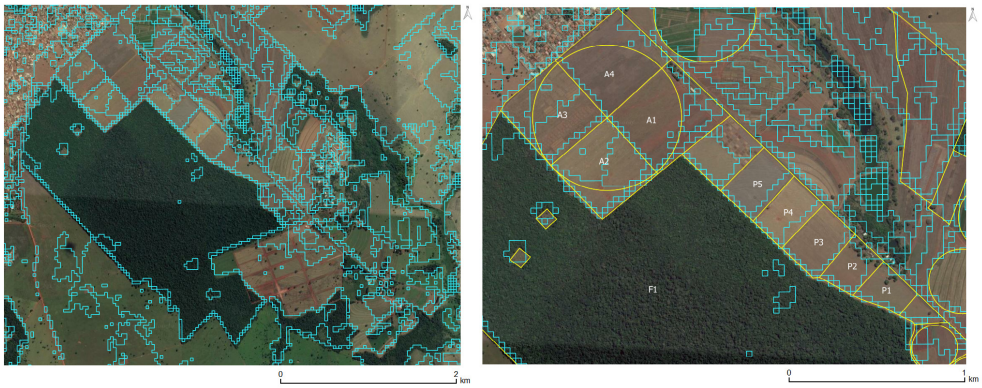

Figure 7. Imagery provided by Google Satellite (left) superimposed with segmentation results (blue outlines). Zoomed area (right) containing the labelled reference polygons (yellow outlines) and the segmented polygons (blue outlines).

Both tests are encouraging and demonstrate the potential of the proposed spatio-temporal segmentation in dealing with time series generated by images of different sensors and spatial resolutions. However, one factor that reduces the quality of the segments is the noise in the time series derived from cloud cover, especially in the second test with Landsat-8 OLI scenes.

Once the proposed method is based on region growing technique, the algorithm contains some disadvantages. Different seed sets, for example, cause different results in segmentation. In addition, there is the dependence of processing order of the seeds, which is particularly noticeable when the regions are small or have some similar properties. In addition, DTW calculation demands a high computational cost.

6. Conclusion

In this paper, we proposed a multitemporal methodology for segmentation of SITS. The use of efficient segmentation algorithms represents an important role because they provide homogeneous regions in space-time and hence simplify the data set. In addition, the spatio-temporal segmentation brings a new way of interpreting data by means of analysing contiguous regions in time. In order to illustrate the potential of the method, we presented two tests on NDVI time series derived from MODIS and Landsat-8 OLI sensors. We compared the segments generated by the proposed algorithm based on photo-interpretation, observing similarities between the segmentation results and reference polygons.

However, the DTW computation and the use of the temporal dimension increases the complexity of processing compared with the segmentation of satellite images which

considers only a single date. Further analysis are needed to apply this approach in regions with higher temporal resolutions and to test different indices and spatial resolutions of Landsat-like image time series.

Acknowledgment

The authors would like to acknowledge the financial support of CAPES, FAPESP e-sensing program (grant 2014/08398-6) and CAPES/COFECUB Programme for the GeoABC Project (n. 845/15) as well as information support of Embrapa National Center for Research on Rice and Beans (CNPAF) and Embrapa LabEx Europe.

References

Adams, R. and Bischof, L. (1994). Seeded region growing. *IEEE Trans. Patt. Anal. Mach. Intell.*, 16(6):641–647.

Bins, L. S., Fonseca, L. M. G., Erthal, G. J., and Ii, F. M. (1996). Satellite imagery segmentation: a region growing approach. *Simpósio Brasileiro de Sensoriamento Remoto*, 8(1996):677–680.

Blaschke, T. (2005). Towards a framework for change detection based on image objects. *Göt. Geo. Abhand.*, 113:1–9.

Blaschke, T. (2010). Object based image analysis for remote sensing. *ISPRS Journ. of Photog. and Remote Sens.*, 65(1):2–16.

Bontemps, S., Bogaert, P., Titeux, N., and Defourny, P. (2008). An object-based change detection method accounting for temporal dependences in time series with medium to coarse spatial resolution. *Remote Sens. of Env.*, 112(6):3181–3191.

Boriah, S. (2010). *Time series change detection: algorithms for land cover change.* PhD thesis, University of Minnesota, 160 p.

Boulila, W., Farah, I. R., Ettabaa, K. S., Solaiman, B., and Ghézala, H. B. (2011). A data mining based approach to predict spatiotemporal changes in satellite images. *International Journal of Applied Earth Observation and Geoinformation*, 13(3):386–395.

Brazil (2011). Sectoral plan for climate mitigation and adaptation. Ministry of agriculture, Livestock and Food Supply. Brasilia.

Bruzzone, L., Smits, P. C., and Tilton, J. C. (2003). Foreword special issue on analysis of multitemporal remote sensing images. *IEEE Trans. Geosci. and Remote Sens.*, 41(11):2419–2422.

Chu, S., Keogh, E., Hart, D., and Pazzani, M. (2002). Iterative deepening dynamic time warping for time series. In *Proceedings of the 2002 SIAM International Conference on Data Mining*, pages 195–212. Society for Industrial and Applied Mathematics, Philadelphia, PA.

De Chant, T. and Kelly, M. (2009). Individual object change detection for monitoring the impact of a forest pathogen on a hardwood forest. *Photogrammetric Engineering & Remote Sensing*, 75(8):1005–1013.

Desclée, B., Bogaert, P., and Defourny, P. (2006). Forest change detection by statistical object-based method. *Remote Sensing of Environment*, 102(1):1–11.

Dey, V., Zhang, Y., and Zhong, M. (2010). A review on image segmentation techniques with remote sensing perspective. *ISPRS*, XXXVIII:31–42.

Drăguţ, L., Csillik, O., Eisank, C., and Tiede, D. (2014). Automated parameterisation for multi-scale image segmentation on multiple layers. *ISPRS*, 88:119–127.

Drăguţ, L., Tiede, D., and Levick, S. R. (2010). ESP: a tool to estimate scale parameter for multiresolution image segmentation of remotely sensed data. *International Journal of Geographical Information Science*, 24(6):859–871.

Duro, D., Franklin, S., and Dubé, M. (2013). Hybrid object-based change detection and hierarchical image segmentation for thematic map updating. *Photog. Eng. & Remote Sens.*, 79(3):259–268.

Eeckhaut, M. V. D., Kerle, N., Poesen, J., and HervÃ¡s, J. (2012). Object-oriented identification of forested landslides with derivatives of single pulse lidar data. *Geomorphology*, 173â174:30–42.

Freitas, R. d., Arai, E., Adami, M., Ferreira, A. S., Sato, F. Y., Shimabukuro, Y. E., Rosa, R. R., Anderson, L. O., and Rudorff, B. F. T. (2011). Virtual laboratory of remote sensing time series: visualization of MODIS EVI2 data set over South America. *Journal of Computational Interdisciplinary Sciences*, 2(1):57–68.

Gómez, C., White, J. C., and Wulder, M. A. (2011). Characterizing the state and processes of change in a dynamic forest environment using hierarchical spatio-temporal segmentation. *Remote Sens. of Env.*, 115(7):1665–1679.

Haralick, R. M. and Shapiro, L. G. (1985). Image segmentation techniques. In *Tec. Symp. East*, pages 2–9, Arlington, VA. Int. Soc. Opt. Photon.

Huete, A., Didan, K., Miura, T., Rodriguez, E. P., Gao, X., and Ferreira, L. G. (2002). Overview of the radiometric and biophysical performance of the modis vegetation indices. *Remote Sens. of Env.*, 83(1):195–213.

Im, J., Jensen, J., and Tullis, J. (2008). Object-based change detection using correlation image analysis and image segmentation. *Int. Journ. of Remote Sens.*, 29(2):399–423.

Jiang, Z., Huete, A. R., Didan, K., and Miura, T. (2008). Development of a two-band enhanced vegetation index without a blue band. *Remote Sens. of Env.*, 112(10):3833–3845.

Justice, C., Townshend, J., Vermote, E., Masuoka, E., Wolfe, R., Saleous, N., Roy, D., and Morisette, J. (2002). An overview of MODIS land data processing and product status. *Remote sensing of Environment*, 83(1):3–15.

Lambin, E. F. and Linderman, M. (2006). Time series of remote sensing data for land change science. *Geoscience and Remote Sensing, IEEE Transactions on*, 44(7):1926–1928.

Maus, V., Câmara, G., Cartaxo, R., Sanchez, A., Ramos, F. M., and Queiroz, G. R. (2016). A time-weighted dynamic time warping method for land-use and land-cover mapping. *IEEE Journ. Sel. Top. in App. Earth Observ. and Remote Sens.*, 9(8):3729–3739.

Niemeyer, I., Marpu, P., and Nussbaum, S. (2008). Change detection using object features. In Blaschke, T., Lang, S., and Hay, G., editors, *Object-Based Image Analysis*,

Lecture Notes in Geoinformation and Cartography, pages 185–201. Springer Berlin Heidelberg.

Oliveira, J. C. d. (2002). Índice para avaliação de segmentação (IAVAS): uma aplicação em agricultura. Master's thesis, Instituto Nacional de Pesquisas Espaciais, 160 p. São José dos Campos.

Pape, A. D. and Franklin, S. E. (2008). MODIS-based change detection for Grizzly Bear habitat mapping in Alberta. *Photog. Eng. & Remote Sens.*, 74(8):973–985.

Petitjean, F., Inglada, J., and Gançarski, P. (2011). Clustering of satellite image time series under time warping. In *Int. Workshop on the Anal. of Multi-temp. Remote Sens.*, pages 69–72, Trento, Italy. IEEE.

Petitjean, F., Inglada, J., and Gançarski, P. (2012). Satellite image time series analysis under time warping. *IEEE Trans. Geosc. and Remote Sens.*, 50(8):3081–3095.

Sakoe, H. and Chiba, S. (1971). A dynamic programming approach to continuous speech recognition. In *Proc. 7th Int. Cong. on Acoust.*, volume 3, pages 65–69, Budapest. Akademiai Kiado.

Sakoe, H. and Chiba, S. (1978). Dynamic programming algorithm optimization for spoken word recognition. In *IEEE Trans. Acoust. Speech and Signal Proc.*, volume 26, pages 43–49, New York, NY. IEEE.

Schiewe, J. (2002). Segmentation of high-resolution remotely sensed data-concepts, applications and problems. *International Archives of Photogrammetry Remote Sensing and Spatial Information Sciences*, 34(4):380–385.

Thompson, J. A. and Lees, B. G. (2014). Applying object-based segmentation in the temporal domain to characterise snow seasonality. *ISPRS*, 97:98–110.

Tucker, C. J. (1979). Red and photographic infrared linear combinations for monitoring vegetation. *Remote Sens. of Env.*, 8(2):127–150.

Tucker, C. J., Pinzon, J. E., Brown, M. E., Slayback, D. A., Pak, E. W., Mahoney, R., Vermote, E. F., and El Saleous, N. (2005). An extended AVHRR 8-km NDVI dataset compatible with MODIS and SPOT vegetation NDVI data. *Int. Journ. of Remote Sens.*, 26(20):4485–4498.